

**AD-A280 117**



AD \_\_\_\_\_

1

**GRANT NO: DAMD17-93-J-3021**

**TITLE: DEVELOPMENT OF METHODS FOR COMPUTER-ASSISTED  
INTERPRETATION OF DIGITAL MAMMOGRAMS FOR EARLY  
BREAST CANCER DETECTION**

**PRINCIPAL INVESTIGATOR: Maryellen L. Giger, Ph.D.**

**CONTRACTING ORGANIZATION: University of Chicago  
5801 South Ellis Avenue  
Chicago, Illinois 60637**

**REPORT DATE: March 24, 1994**

**TYPE OF REPORT: Annual Report**

**DTIC  
ELECTE  
JUN 13 1994  
S F D**

**PREPARED FOR: U.S. Army Medical Research, Development,  
Acquisition and Logistics Command (Provisional),  
Fort Detrick, Frederick, Maryland 21702-5012**

**DISTRIBUTION STATEMENT: Approved for public release;  
distribution unlimited**

**The views, opinions and/or findings contained in this report are  
those of the author(s) and should not be construed as an official  
Department of the Army position, policy or decision unless so  
designated by other documentation.**

**94-17971**



**DTIC QUALITY INSPECTED 1**

**94 6 10 077**

**REPORT DOCUMENTATION PAGE**Form Approved  
OMB No. 0704-0188

Public reporting burden for this collection of information is estimated to average 1 hour per response, including the time for reviewing instructions, searching existing data sources, gathering and maintaining the data needed, and completing and reviewing the collection of information. Send comments regarding this burden estimate or any other aspect of this collection of information, including suggestions for reducing this burden, to Washington Headquarters Services, Directorate for Information Operations and Reports, 1215 Jefferson Davis Highway, Suite 1204, Arlington, VA 22202-4302, and to the Office of Management and Budget, Paperwork Reduction Project (0704-0188), Washington, DC 20503.

<b>1. AGENCY USE ONLY (Leave blank)</b>		<b>2. REPORT DATE</b> 24 March 1994	<b>3. REPORT TYPE AND DATES COVERED</b> Annual Report (3/1/93 - 2/28/94)	
<b>4. TITLE AND SUBTITLE</b> Development of Methods for Computer-Assisted Interpretation of Digital Mammograms for Early Breast Cancer Detection			<b>5. FUNDING NUMBERS</b>  Grant No. DAMD17-93-J-3021	
<b>6. AUTHOR(S)</b>  Maryellen L. Giger, Ph.D.				
<b>7. PERFORMING ORGANIZATION NAME(S) AND ADDRESS(ES)</b> University of Chicago 5801 South Ellis Avenue Chicago, Illinois 60637			<b>8. PERFORMING ORGANIZATION REPORT NUMBER</b>	
<b>9. SPONSORING/MONITORING AGENCY NAME(S) AND ADDRESS(ES)</b> U.S. Army Medical Research, Development, Acquisition and Logistics Command (Provisional), Fort Detrick, Frederick, Maryland 21702-5012			<b>10. SPONSORING/MONITORING AGENCY REPORT NUMBER</b>	
<b>11. SUPPLEMENTARY NOTES</b>				
<b>12a. DISTRIBUTION / AVAILABILITY STATEMENT</b>  Approved for public release; distribution unlimited			<b>12b. DISTRIBUTION CODE</b>	
<b>13. ABSTRACT (Maximum 200 words)</b>  The goal of the research is to develop a computer-vision module as an aid to radiologists. The specific aims are: (1) Further development of advanced computerized schemes for the detection and classification of masses and microcalcifications in digital mammograms, including quantitative analysis of the radiographic characteristics and the decision-making processes used by radiologists in making a decision with respect to the likelihood of malignancy and choosing the appropriate course of action. (2) Development of a dedicated "intelligent" modular system with man-machine interfaces and fast computation times appropriate for the effective use of the computer-vision schemes. (3) Evaluation of the efficacy and efficiency of the module using a large clinical database. The significance of this research is that if the detectability of cancers can be increased by employing a computer to aid the radiologist's diagnosis, then the treatment of patients with cancer can be initiated earlier and their chance of survival improved. Systematic introduction of computer-vision tools to radiologists that is presented in this proposal requires minimal modification to the current reading habits of radiologists. When digital mammographic imaging units become commonplace, the computer-vision module can be interfaced to electronic, filmless medical imaging reading areas.				
<b>14. SUBJECT TERMS</b> Computer-aided diagnosis, computer vision, breast cancer, mammography			<b>15. NUMBER OF PAGES</b>	
			<b>16. PRICE CODE</b>	
<b>17. SECURITY CLASSIFICATION OF REPORT</b>  Unclassified	<b>18. SECURITY CLASSIFICATION OF THIS PAGE</b>  Unclassified	<b>19. SECURITY CLASSIFICATION OF ABSTRACT</b>  Unclassified	<b>20. LIMITATION OF ABSTRACT</b>  Unlimited	

## FOREWORD

Opinions, interpretations, conclusions and recommendations are those of the author and are not necessarily endorsed by the US Army.

Where copyrighted material is quoted, permission has been obtained to use such material.

Where material from documents designated for limited distribution is quoted, permission has been obtained to use the material.

Citations of commercial organizations and trade names in this report do not constitute an official Department of Army endorsement or approval of the products or services of these organizations.

In conducting research using animals, the investigator(s) adhered to the "Guide for the Care and Use of Laboratory Animals," prepared by the Committee on Care and Use of Laboratory Animals of the Institute of Laboratory Resources, National Research Council (NIH Publication No. 86-23, Revised 1985).

For the protection of human subjects, the investigator(s) adhered to policies of applicable Federal Law 45 CFR 46.

In conducting research utilizing recombinant DNA technology, the investigator(s) adhered to current guidelines promulgated by the National Institutes of Health.

In the conduct of research utilizing recombinant DNA, the investigator(s) adhered to the NIH Guidelines for Research Involving Recombinant DNA Molecules.

In the conduct of research involving hazardous organisms, the investigator(s) adhered to the CDC-NIH Guide for Biosafety in Microbiological and Biomedical Laboratories.

Accession For	
NTIS CRA&I	<input checked="checked" type="checkbox"/>
DTIC TAB	<input type="checkbox"/>
Unannounced	<input type="checkbox"/>
Justification .....	
By .....	
Distribution /	
Availability Codes	
Dist	Avail and/or Special
A-1	

*Manjellen Legin* 3/24/94  
PI - Signature Date

## Table of Contents

	Page
<b>INTRODUCTION</b> .....	<b>5</b>
Nature of the problem	
Background of previous work	
Purpose of the present work	
Methods of approach	
<b>BODY</b> .....	<b>14</b>
(1) Development of the computerized schemes for the detection and classification of masses and microcalcifications	
Experimental methods	
(a) Development of the computerized detection scheme for masses	
Results to date	
(b) Development of the detection scheme for microcalcifications	
Results to date	
(c) Development of computerized classification schemes	
Results to date: classification of masses	
Results to date: classification of microcalcifications	
(2) Development of a dedicated CAD module for use by radiologists	
Experimental methods	
Results to date	
(3) Evaluation procedure using large clinical databases	
Experimental methods	
Results to date	
<b>CONCLUSIONS</b> .....	<b>33</b>
<b>REFERENCES</b> .....	<b>35</b>

## INTRODUCTION

### Nature of the problem

Breast cancer is a leading cause of death in women, causing an estimated 44,000 deaths per year (1). Mammography is the most effective method for the early detection of breast cancer (2-5) and it has been shown that periodic screening of asymptomatic women does reduce mortality (6-11). Various medical organizations have recommended the use of mammographic screening for the early detection of breast cancer (3). Thus, mammography is becoming one of the largest volume x-ray procedures routinely interpreted by radiologists.

It has been reported that between 30 to 50% of breast carcinomas detected mammographically demonstrate clusters of microcalcifications (12-14), although about 80% of breast carcinomas reveal microcalcifications upon microscopic examination (15-18). In addition, studies indicate that 26% of nonpalpable cancers present mammographically as a mass while 18% present both with a mass and microcalcifications (19). Although mammography is currently the best method for the detection of breast cancer, between 10-30% of women who have breast cancer and undergo mammography have negative mammograms (20-24). In approximately two-thirds of these false-negative mammograms, the radiologist failed to detect the cancer that was evident retrospectively (23-26). Low conspicuity of the lesion, eye fatigue and inattentiveness are possible causes for these misses. We believe that the effectiveness (early detection) and efficiency (rapid diagnosis) of screening procedures could be increased substantially by use of a computer system that successfully aids the radiologist by indicating locations of suspicious abnormalities in mammograms.

Many breast cancers are detected and referred for surgical biopsy on the basis of a radiographically detected mass lesion or cluster of microcalcifications. Although general rules for the differentiation between benign and malignant breast lesions exist (20,27), considerable misclassification of lesions occurs with the current methods. On average, only 10-30% of masses referred for surgical breast biopsy are actually malignant (20,28). Surgical biopsy is an invasive technique that is an expensive and traumatic experience for the patient and leaves physical scars that may hinder later diagnoses (to the

extent of requiring repeat biopsies for a radiographic tumor-simulating scar). A computerized method capable of detecting and analyzing the characteristics of benign and malignant masses, in an objective manner, should aid radiologists by reducing the numbers of false-positive diagnoses of malignancies, thereby decreasing patient morbidity as well as the number of surgical biopsies performed and their associated complications.

The development of computer methods to assist radiologists is a timely project in the sense that digital radiography is on the threshold of widespread clinical use. The arrival of digital radiographic systems allows for the acquisition of image data in a format accessible to computerized schemes. The potential significance of this research project lies in the fact that if the detectability of cancers can be increased by employing a computer to aid the radiologist's diagnosis, then the treatment of patients with cancer can be initiated earlier and their chance of survival improved.

The systematic and gradual introduction of computer-assisted interpretation to radiologists that is presented in this proposal is very important in that it allows for a mode of presentation with minimum modification to the current reading habits of radiologists and does not require a "digital" department in which reading must be done from a CRT screen. These two issues are of concern since (1) some radiologists are not comfortable with computer-based methods and (2) primary diagnosis from a CRT display is still controversial. However, the introduction of computer vision to radiologists presented in this proposal is not affected by either concern. In addition, when filmless image acquisition and/or digital (PACS) radiology departments are commonplace in the future, the computer-vision module can be immediately interfaced to electronic, filmless imaging and reading areas.

### **Background of previous work**

In the 1960's and 70's, several investigators attempted to analyze mammographic abnormalities with computers. Winsberg et al. (29), in an early study, examined areas of increased density in contralateral breasts. They felt that their results demonstrated the feasibility for future computer interpretation of mammograms. Spiesberger (30) developed various feature-extraction techniques and a two-view verification method involving medio-lateral oblique and cranio-caudal views to detect

microcalcifications. Kimme et al. (31) developed a computerized method for the detection of suspicious abnormalities in mammograms based on the statistical measures of textural features. They tested their algorithm on 7 patient cases. A similar approach using texture analysis and bilateral comparison was also employed by Hand et al (32) and Semmlow (33) in the computerized localization of suspicious abnormal areas of breasts. Their results yielded a 66% true-positive rate with approximately 26 false suspicious areas per image. With regard to classification methods, Ackerman et al. (34), using digital xeroradiographs, devised four measures of malignancy: calcification, spiculation, roughness and shape, to perform classification on specific areas selected by human observers. The authors viewed their research as only a small step toward the automated reading of xeroradiographs and appeared to discontinue prematurely their computer vision work. The same group (35) did, however, attempt to improve diagnosis by using 36 radiographic properties which were evaluated semi-quantitatively by a radiologist for input to a computer decision tree. Wee et al. (36) and Fox et al. (37) performed preliminary studies on the classification of microcalcifications. These previous studies demonstrated the potential capability of using a computer in the detection of mammographic abnormalities. Their results, however, yielded a large number of false-positives and were based on small data sets.

Computer-aided diagnosis, in general, has attracted little attention during the last decade, perhaps due to the inconvenience involved in obtaining a radiograph in digital format. Recent work, though, shows a promising future. Magnin et al. (38) and Caldwell (39) used texture analysis to evaluate the breast's parenchymal pattern as an indicator of cancer risk. These preliminary studies raised many unanswered questions regarding topics ranging from the digital recording process to the type of numerical risk coefficient employed. Thus, further studies using texture analysis are indicated. The work by Fam and Olson (40,41) on the computer analysis of mammograms is encouraging; however, their method has only been tested on 20 mammographic regions of interest (each roughly half a mammogram). Davies and Dance (42) have reported on their automatic method for the detection of clustered calcifications using local gray-level thresholding and also a clustering rule. Their results yielded a true-positive rate of 96%; however, no indications of the subtlety and size of the calcifications were given. Astley et al. (43), Grimaud et al. (44) and Jin et al. (45) recently reported on their methods

for the detection of breast lesions. Karssemeijer (46) has described a stochastic method based on Bayesian decision theory that appears promising. Lai et al. (47) and Brzakovic et al. (48) are also developing techniques for the detection of mass lesions. The actual performance level and difficulty of the databases, however, are unknown. Gale et al. (49) and Getty et al. (50) are both developing computer-based classifiers, which take as input diagnostically-relevant features obtained from radiologists' readings of breast images. Getty et al. found that with the aid of the classifier, community radiologists performed as well as unaided expert mammographers in making benign-malignant decisions. Swett et al. (51,52) are developing an expert system to provide visual and cognitive feedback to the radiologist using a critiquing approach combined with an expert system. The system has been demonstrated, though not tested.

We in the Kurt Rossmann Laboratories for Radiologic Image Research at The University of Chicago have vast experience in developing various computer-aided diagnosis (CAD) methods in mammography, chest radiography, and angiography (53-66). We believe that our CAD methods in digital mammography, which include the computerized detection of microcalcifications and masses, have achieved levels of sensitivity and specificity that warrant testing in a clinical environment.

Our detection scheme for clustered microcalcifications includes a preprocessing step referred to as a difference-image approach (53,54). Basically, the original digital mammogram is spatially filtered twice: once to enhance the signal-to-noise ratios of the microcalcifications and a second time to suppress them. The difference between the two resulting processed images yields an image (a difference image) in which the variations in background density are largely removed.

Microcalcifications are then segmented from the difference image using global gray-level thresholding and local thresholding techniques. The segmented image is next subjected to feature-extraction techniques in order to remove signals that likely arise from structures other than microcalcifications. An area filter (56), based on mathematical morphology, is used to eliminate small features. Next, each region of interest that contains remaining features is subjected to low-frequency background correction and is characterized by the first moment of its power spectrum, defined as the weighted average of radial spatial frequency over the two-dimensional power spectrum (55). A clustering filter



(57) is next used so that only clusters that contain more than a preselected number of signals within a region of preselected size are retained by the computer. The computerized scheme, using 78 mammograms (39 normal and 39 abnormal) in which most clusters were quite subtle, the scheme yielded a sensitivity of 85% with approximately 2.5 false-positive detections per image (58).

The computerized scheme for detection of clustered microcalcifications (55) developed at The University of Chicago has been tested as an aid to radiologic diagnosis. Using a database of 60 clinical mammograms, half of which contained subtle clusters of microcalcifications, a human observer study was conducted in order to examine the effect of the computer-vision aid on radiologists' performance in a situation that simulated rapid interpretation of screening mammograms. The computer scheme attained an 87% true-positive detection rate with an average of four false-positive clusters per image. The effect of the number of false-positive detections on radiologist performance was also examined by simulating a computer performance level of 87% sensitivity with one false-positive detection per image. Radiologist detection performance was evaluated using ROC (receiver operating characteristic) methodology (68). It was found from the ROC analysis that there was a statistically significant improvement in the radiologists' accuracy when they were given the computer-generated diagnostic information (at either false-positive level), compared with their accuracy obtained without the computer output.

Our scheme for the detection of mammographic masses is based on deviations from the architectural symmetry of normal right and left breasts, with asymmetries indicating potential masses (60,61). The input to the computerized scheme, for a given patient, are the four conventional mammograms obtained in a routine screening examination: the right cranio-caudal (CC) view, the left CC view, the right medio-lateral-oblique (MLO) view, and the left MLO view. After automatic registration of corresponding left and right breast images, a nonlinear subtraction technique is employed in which gray-level thresholding is performed on the individual mammograms prior to subtraction. Ten images thresholded with different cutoff gray levels are obtained from the right breast image, and ten are obtained from the left breast image. Next, subtraction of the corresponding right and left breast images is performed to generate ten bilateral-subtraction images. Run-length

analysis is then used to link the data in the various subtracted images. This linking process accumulates the information from a set of 10 subtraction images into two images that contain locations of suspected masses for the left and right breasts. Next, feature-extraction techniques, which include morphological filtering and analysis of size, shape and distance from border, are used to reduce the number of false-positive detections. Currently, using 150 pairs of clinical mammograms (from 75 cases), the approach achieves a true-positive detection rate of approximately 85% with 3 to 4 false-positive detections per image (62).

We have also investigated the application of artificial neural networks to the detection and classification of mammographic lesions. We used an artificial neural network (ANN) to extract microcalcification image data from digital mammograms (59). The ANN, which was supplied with the power spectra of remaining suspected regions (from the CAD scheme) as input, distinguished actual clustered microcalcifications from false-positive regions and was able to eliminate many of the false positives. Also, we are applying ANNs to the decision-making task in mammography (63). Three-layer, feed-forward neural networks with a back-propagation algorithm were trained for the interpretation of mammograms based on features extracted from mammograms by experienced radiologists. The database for input to the ANN consisted of features extracted from 133 textbook cases and 60 clinical cases. Performance of the ANN was evaluated by ROC analysis. In tests, using 43 initial image features (related to masses, microcalcifications and secondary abnormalities) that were later reduced to 14 features, the performance of the neural network was found to be higher than the average performance of attending and resident radiologists in classifying benign and malignant lesions. At an optimal threshold for the ANN output value, the ANN achieved a classification sensitivity of 100% for malignant cases with a false-positive rate of only 41%, whereas the average radiologist yielded a sensitivity of only 89% with a false-positive rate for classification of 60%.

We are also developing computer-aided methods for the interpretation of digital chest radiographs, such as in the detection of pulmonary nodules, interstitial infiltrates, pneumothorax and cardiomegaly (67,69-75). The computer-vision scheme for the detection of lung nodules is based on a difference-image approach, which (like the one described above for detection of clustered

microcalcifications) is novel in that it attempts to remove the structured anatomic background before applying feature-extraction techniques. After the difference between the signal-enhanced image and the signal-suppressed image is obtained, gray-level thresholding and feature-extraction techniques (involving the size, contrast and shape of the detected features) are performed by the computer to identify the locations of possible nodules. More recently, false-positive detections have been reduced by adding nonlinear filters to the difference-image step and additional feature-extraction techniques based on detailed analyses of the false positives.

The research team in the Rossmann Lab also has considerable experience in evaluation of factors affecting image quality and diagnostic accuracy in digital radiography. We have investigated basic imaging properties including the characteristic system response, spatial resolution properties and noise properties of various types of digital radiographic imaging systems (76-86). The effects of various physical parameters, such as detector system, sampling aperture, pixel size, number of quantization levels, exposure level and display aperture, were examined at various stages of the digital imaging chain (87-91). Knowledge gained in this research will be useful in understanding the effect of spatial resolution and noise on the performance of computer-assisted interpretation.

In developing methods for computer-assisted interpretations, it is crucial to employ appropriate means for evaluation. We have carried out various observer performance studies in comparing the detection capability of new techniques both with regard to simulated and clinical images. 18-alternative forced-choice observer studies were employed to examine the effect of pixel size on the threshold contrast of simple objects digitally superimposed on uniform background noise (92-94) and the effect of structured background on the detectability of simulated stenotic lesions (95). In an observer study with radiologists using clinical images, ROC analysis was employed in order to examine the effects of different display modalities (film and CRT) on diagnostic accuracy in digital chest radiography (96). Similar studies were performed to investigate the effect of data compression ratios on detectability (97), the comparison of computed radiography with conventional screen/film imaging (98), and the utility of computer-assisted interpretation in mammography (55) and chest (71). In addition, we have used ROC and FROC analyses to evaluate the performance level of the computerized schemes and the artificial

neural networks (99). This broad experience will provide the basis for developing similar methodology to evaluate the computer-vision modules for mammography proposed in this application.

### **Purpose of the present work**

The main hypothesis to be tested is that given a dedicated computer-vision module for the computer-assisted interpretation of mammograms, the diagnostic accuracy for mammographic interpretation will be improved, yielding earlier detection of breast cancer (i.e., a reduction in the number of missed lesions) and a reduction in the number of benign cases sent to biopsy.

Computer-aided diagnosis (CAD) can be defined as a diagnosis made by a radiologist who takes into consideration the results of a computerized analysis of radiographic images and uses them as a "second opinion" in detecting lesions and in making diagnostic decisions. The final diagnosis would be made by the radiologist. Although mammography is currently the best method for the detection of breast cancer, between 10-30% of women who have breast cancer and undergo mammography have negative mammograms (20-24). It has been suggested that double reading (by two radiologists) may increase sensitivity (100-102). Thus, one aim of CAD is to increase the efficiency and effectiveness of screening procedures by using a computer system, as a "second opinion or second reading," to aid the radiologist by indicating locations of suspicious abnormalities in mammograms.

If a suspicious region is detected by a radiologist, he or she must then visually extract various radiographic characteristics. Using these features, the radiologist then decides if the abnormality is likely to be malignant or benign, and what course of action should be recommended (i.e., return to screening, return for follow-up or send for biopsy). Many patients are referred for surgical biopsy on the basis of a radiographically detected mass lesion or cluster of microcalcifications. On average, only 10-20% of masses referred for surgical breast biopsy are actually malignant (20,28). Thus, another aim of CAD is to extract and analyze the characteristics of benign and malignant lesions in an objective manner in order to aid the radiologist by reducing the numbers of false-positive diagnoses of malignancies, thereby decreasing patient morbidity as well as the number of surgical biopsies performed and their associated complications

## **Methods of approach**

The objective of the proposed research is to develop a dedicated computer-vision module for use in mammography in order to increase the diagnostic decision accuracy of radiologists and to aid in mammographic screening programs. The computer-aided diagnostic module will incorporate various novel computer-vision and artificial intelligence schemes already under development in the Rossmann Laboratories at the University of Chicago.

The specific objectives of the research to be addressed are:

(1) Further development of advanced computerized schemes for the detection and classification of masses and microcalcifications in digital mammograms. This part of the research involves quantitative analysis of the radiographic characteristics of masses and microcalcifications, and the decision-making processes used by radiologists in making a decision with respect to the likelihood of malignancy and in choosing the appropriate course of action.

(a) Further development of an advanced computerized detection scheme for masses that uses bilateral-subtraction techniques, gray-level thresholding, and analysis of various image features.

(b) Further development of an advanced computerized detection scheme for microcalcifications that uses linear and nonlinear spatial filters, spectral content analysis and various morphological filters for size, contrast and cluster analyses.

(c) Further development of advanced computerized classification schemes for masses and microcalcifications that use computer-vision techniques and artificial-intelligence techniques to calculate a probability of malignancy.

(2) Development of a dedicated module with man-machine interfaces appropriate for the effective and efficient use of the CAD schemes. Final diagnostic decisions will remain with the radiologists.

(a) Optimization of the CAD software.

(b) Examination of various methods of presenting the computer's results to the radiologist.

(c) Development of a prototype intelligent modular workstation using a high-speed (fast CPU & large-capacity memory) computer and a high-resolution, filmless CRT display.

(3) Evaluation of the efficacy and efficiency of the dedicated computer-vision module for mammography using a large clinical database. This part will use both film and filmless media for image acquisition and display.

**BODY: Experimental methods and results to date**

(1) Development of the computerized schemes for the detection and classification of masses and microcalcifications in digital mammograms.

**Experimental methods**

The computerized schemes for detection and classification are at various levels of development. These schemes will be used as aids by radiologists in the interpretation of mammograms. For the development and testing of these algorithms, we will collect 500 mammographic cases from the Department of Radiology. Initially, these cases will include screen/film mammograms that are currently acquired in the department. Later, the database will include digital images both from computed radiography (CR) units (stimulable phosphor) and from a CCD array detector that will be installed on our digital biopsy unit (see Section 6 on Facilities).

**(a) Development of the computerized detection scheme for masses.**

The computer-vision scheme is based on deviations from the architectural symmetry of normal right and left breasts, with asymmetries indicating potential masses (60-62). Thus, we will continue investigating subtraction techniques as a means to increase the conspicuity of masses in mammograms. These techniques will be combined with analysis of individual mammograms. The input to the computerized scheme, for a given patient, are the four conventional breast images obtained in a routine screening examination: the right CC view, the left CC view, the right MLO view, and the left MLO view. Mammograms will be digitized using a laser scanner digitizer (2K by 2K matrix). In the initial detection stage, the digital image can be reduced to a 512 by 512 matrix (with an effective pixel size of

0.4 mm) due to the large size of masses relative to the pixel size. An automated alignment technique, which we have developed, will be used to align corresponding left and right breast images and also images of the same breast obtained over some time period. The automated alignment of two corresponding breast images will be performed in three stages: image segmentation, image feature selection and image registration. During image segmentation, the breast area will be isolated from the exterior region using a technique which combines multiple gray-level thresholding and morphological filtering. With image-feature selection, landmarks on each breast image will be determined. These landmarks are the breast border and the nipple position. Since the image features around the nipple often include a thicker skin line and greater subcutaneous parenchymal opacity, a band signature method will be employed to identify the nipple position along the breast border. During image registration, translation and rotation of one of the breast images relative to the other will be determined using a partial-border matching technique.

Once the two images are aligned relative to each other, the detection of possible asymmetries between the border-matched right and left breast images is achieved by correlation of the two mammograms, using a bilateral-subtraction technique. We are investigating linear and nonlinear subtraction methods. With linear subtraction, the two breast images are subtracted (using a left-minus-right convention) and then gray-level thresholding is performed in order to segment the image into possible locations of suspect masses. With the nonlinear technique, gray-level thresholding is performed prior to subtraction. This initial thresholding eliminates some normal anatomic background from further analysis. A selected number of images thresholded with different cutoff gray levels is obtained from the right breast image, and a corresponding number is obtained from the left breast image. Subtraction of ten sets of corresponding right and left breast images, each thresholded at ten different levels, is performed to generate ten bilateral-subtraction images (containing information on suspicious masses in the two original mammograms). A linking process then accumulates the information into two images, called runlength images, where the value of each pixel in each image indicates how often the corresponding location in the set of 10 subtraction images has gray levels above

or below a particular cutoff gray value. These images are next thresholded to yield the suspicious areas and submitted for feature extraction.

Feature-extraction techniques will be performed on both the runlength images and the original mammograms to reduce the number of false-positive detections. Initially, a morphological closing operation followed by an opening operation will be used to eliminate isolated pixels and merge small neighboring features. Next a size test will be used to eliminate features that are smaller than a predetermined cutoff size. A border test will be used to eliminate artifact features arising from any border misalignment that occurred during digitization and registration. On the original images, suspected regions will be subjected to region-growing techniques and then examined with respect to size, shape and contrast, in order to eliminate features of elongated shape and diffuse connective tissue.

Further analysis will be performed by correlating geometrically the information obtained from the CC mammographic pair and the MLO pair. Since the two views are obtained from the same breast image, the appearance of a mass in one view of a breast will be expected to exist in the other view of the same breast. This geometric correlation will need to take into account the different angles of projection of the 3-dimensional breast in forming the two 2-dimensional images and the possibly different amounts of physical compression applied to the breast in question during acquisition of the two views.

In addition to comparing the right and left breast images of a given view obtained at a given time, comparisons will be made between images of the same breast obtained at the same projection but at different times in order to note changes in the breast. This follows the methodology employed by mammographers when interpreting a case with previous examinations available. Similar subtraction techniques and feature-extraction methods will be employed. Use of histogram specification methods (103), however, may be necessary in order to match the gray-level distributions of the two images (that were obtained at different times) when there exists a large variation in the exposure techniques employed.



## **Results to date**

Currently, the scheme employs two pairs of conventional screen-film mammograms (the right and left MLO views and CC views), which are digitized. After the right and left breast images in each pair are aligned, a nonlinear bilateral-subtraction technique is employed that involves linking multiple subtracted images to locate initial candidate masses. Various features are then extracted and merged using an artificial neural network in order to reduce false-positive detections resulting from the bilateral subtraction.

The features extracted from each suspected mass lesion include geometric measures, gradient-based measures and intensity-based measures. The geometric measures are lesion size, lesion circularity, margin irregularity, and lesion compactness. The gradient-based measures are the average gradient (based on a 3 by 3 Sobel operator) and its standard deviation calculated within the specified region of interest. The intensity-based measures are local contrast, average gray value, standard deviation of the gray values within the lesion, and the ratio of the average to the standard deviation. The features were normalized between 0 and 1 and input to the a back-propagation, feed-forward neural network. The ANN's structure consisted of 10 input units, one hidden layer with 7 hidden units and one output unit. In this task, the output unit ranged from 0 to 1, where 1 corresponded to the suspected lesion being an actual mass (i.e., a true-positive detection) and 0 corresponded to the suspected lesion being a false-positive detection (and thus, allowed to be eliminated as a suspect lesion-candidate). Based on the performances of the ANN as a function of iteration, in terms of self-consistency and round robin analyses, the optimal number of training iterations was determined.

ROC (receiver operating characteristic) analysis was applied to evaluate the output of the ANN in terms of its ability to distinguish between actual mass lesions and false-positive detections. The output values from the ANN for actual masses and for false-positive detections were used in the ROC analysis as the decision variable. Basically, the ROC curve represents the true-positive fraction and the false-positive fraction at various thresholds of the ANN output. ROC analysis was used as an index of performance in determining the "optimal" number of input features, the "optimal" number of hidden units, and the "optimal" number of training iterations of the ANN.

In the self-consistency analysis, the ANN achieved an Az of 1.0 and in the round-robin analysis, the ANN achieved an Az of 0.92 in distinguishing actual masses (true positives) from false-positive detections. In an evaluation study using the 154 pairs of clinical mammograms (90 pairs with masses and 64 pairs without), the detection scheme yielded a sensitivity of 95% at an average of 2.5 false-positive detections per image. This is a substantial improvement from the previous year's performance of 85% sensitivity and 4 false-positive detections per image.

**(b) Development of the computerized detection scheme for microcalcifications.**

Microcalcifications are a primary indicator of cancer and are often visible in the mammogram before a palpable tumor can be detected. Initially, clinical screen/film mammograms will be digitized using the laser scanner and analyzed in the 2048 by 2048 matrix format in order to retain the high spatial-frequency content of the microcalcifications. First, the original mammograms will be processed to enhance and suppress the signal of the microcalcifications, followed by calculation of a difference image. Both linear and nonlinear filters will be investigated for enhancement and suppression. Previous use of both linear and nonlinear filters in detecting lung nodules in digital chest images has shown that while both types of filters tended to detect nodules, locations of false positives differed. Thus, a combination of the results from each processing technique has the potential to yield high sensitivity and reduce the number of false-positive detections. Examples of filters for signal enhancement include a linear "matched" filter that matches the profile of a typical microcalcification and a morphological open filter (to enlarge the appearance of microcalcifications). Morphological filtering (104) is basically a nonlinear filtering method that calculates the logical AND (erosion function) or OR (dilation function) of pixels within a kernel of some given size and shape. When extended to gray-scale images, the logical AND and OR operations can be replaced by minimum and maximum operations. By appropriately choosing the size and shape of the kernels, as well as the sequences of the AND and the OR, the filters can eliminate groups of pixels of limited size or merge neighboring pixels. Examples of filters for signal suppression include ring-shaped filters that yield either the average or median value of the surrounding normal anatomic background (54).

The difference image will then be subjected to various feature-extraction techniques to reduce further the number of false-positive detections. These techniques will test for size, contrast and spectral content of neighboring features. New methods for analyzing these features will involve the use of morphological filters. For example, we have found that the use of asymmetric morphological filters to eliminate features less than 3 pixels in size are more effective and efficient than use of a point-by-point analysis that involves counting the number of pixels in each remaining feature and comparing it to a size cutoff. In addition, the presence of clustering of the microcalcifications will be examined since singular microcalcifications are usually not cancerous. The morphological kernel for the clustering test will correspond to the size of a typical cluster (approximately 6 mm in diameter).

### **Results to date**

The microcalcification detection scheme consists of three steps. First, the image is filtered so that the signal-to-noise ratio of microcalcifications is increased by suppression of the normal background structure of the breast. Second, potential microcalcifications are extracted from the filtered image with a series of three different techniques: a global thresholding based on the grey-level histogram of the full filtered image, an erosion operator for eliminating very small signals, and a local adaptive grey-level thresholding. Third, some false-positive signals are eliminated by means of a texture analysis technique, and a nonlinear clustering algorithm is then used for grouping the remaining signals.

In our computer detection scheme it is necessary to group or cluster microcalcifications, since clustered microcalcifications are more clinically significant than are isolated microcalcifications. In the past we used a "growing" technique in which signals (possible microcalcifications) were clustered by grouping those that were within some predefined distance from the center of the growing cluster. In this paper, we introduce a new technique for grouping signals, which consists of two steps. First, signals that may be several pixels in area are reduced to single pixels by means of a recursive transformation. Second, the number of signals (non-zero pixels) within a small region, typically  $3.2 \times 3.2$  mm, are counted. Only if three or more signals are present within such a region are they preserved in the output image. In this way, isolated signals are eliminated. Furthermore, this method

can eliminate falsely detected clusters, which were identified by our previous detection scheme, based on the spatial distribution of signals within the cluster. The differences in performance of our CAD scheme for detecting clustered microcalcifications using the old and new clustering techniques was measured using 78 mammograms, containing 41 clusters. The new clustering technique improved our detection scheme by reducing the false-positive detection rate while maintaining a sensitivity of approximately 85%.

We also applied artificial neural networks to the differentiation of actual "true" clusters of microcalcifications from normal parenchymal patterns and from false positive detections as reported by a computerized scheme. The differentiation was carried out in both the spatial and spatial frequency domains. In the spatial domain, the performance of the neural networks was evaluated quantitatively by means of ROC analysis. We found that the networks could distinguish clustered microcalcifications from normal nonclustered areas in the frequency domain, and that they could eliminate approximately 50% of false-positive clusters of microcalcifications while preserving 95% of the positive clusters.

The number of false-positive detections was even further reduced when a shift-invariant artificial neural network (SIANN) was used to analyze the remaining suspected locations. The SIANN is a multilayer back-propagation neural network with local, shift-invariant interconnections. The advantage of the SIANN is that the result of the network is not dependent on the locations of the clustered microcalcifications in the input layer. The performance of the SIANN was evaluated by means of a jack-knife method and ROC analysis using a database of 168 regions as reported by the CAD scheme. Approximately 55% of the false positives were eliminated without loss of any of the true-positive detections. We also examined the effect of the network structure on the performance of the SIANN. These techniques led to a performance of 85% sensitivity with approximately 0.7 false-positive detections per image.

#### **(c) Development of computerized classification schemes.**

Various feature-extraction techniques and artificial intelligence schemes will be investigated in order to distinguish malignant masses and/or microcalcifications from benign masses and/or

microcalcifications. The database for this investigation will be obtained from the conventional four screening breast images, as well as special views such as spot compression.

In our previous work, we compiled a list of features that radiologists use in distinguishing between malignant and benign masses. These features include: margin spiculation (number of spiculations, length of spiculation, and difference between spicules and local linear features), shape (linear to spherical, geometrical to diffuse, and existence of satellite lesions), size (mean diameter), margin characteristics (complete to inseparable from surround, well-defined to indistinct, and presence of halo sign), and pattern of interior (uniformity, presence of well-defined lucencies, and opacity relative to size). The analysis of spiculation will be based on a novel computer-vision method involving the Fourier analysis of the fluctuations around the margin of the mass in question (60). The computer-extracted margin used in the analysis for spiculation also contains information related to the number and length of spiculations. Also, prior to the analysis of spiculation, the mass is extracted from the normal anatomic background of the breast parenchyma. Currently, region-growing techniques are employed for this extraction. Once extracted, the shape and size of the mass can be easily calculated. The size will be defined as the effective diameter of a circle that has the same area as the extracted mass. The shape will be expressed by a degree of circularity, which will be defined as the ratio of the area of the mass within the equivalent circle to the total area of the mass. Masses with ill-defined margins are more likely to be malignant than those with relatively well-defined margins. Thus, a margin gradient test will be developed to measure the sharpness of the margin. This sharpness will be defined as the degree of density change across the margin and will be measured perpendicular to the margin at all points along the margin. The pattern of the interior will be quantitatively determined from the spectral content of the interior.

Features related to the classification of microcalcifications include: the shape of the individual microcalcifications (rounded to irregular, linear, and branched), uniformity of microcalcifications within a cluster (uniformity in size, shape, and density), distribution of the microcalcifications (diffuseness and shape of cluster) and presence of macrocalcifications. The size and shape of the individual microcalcifications will be determined by the computer using an effective diameter and a circularity

measure, respectively, as described earlier. Uniformity within a cluster will be assessed by calculating the spread of values for a particular characteristic such as size. Once a cluster has been defined, its diffuseness will be given by the number of microcalcifications per unit area and its shape will be defined using a circularity measure.

These various computer-determined quantitative measures describing the mass or cluster of microcalcifications in question will be input to an artificial neural network that will merge the features into a probability of malignancy for use by radiologists. As mentioned in the Background section, our work with a neural network in merging human-reported mammographic features into a malignant/benign decision has been extremely promising. The input data (corresponding to the computer-extracted features of the masses and microcalcifications) will be represented by numbers ranging from 0 to 1 and will be supplied to the input units of the neural network. The output data from the neural network is then provided from output units through two successive nonlinear calculations in the hidden and output layers. The calculation at each unit in a layer includes a weighted summation of all entry numbers, an addition of a certain offset number, and a conversion into a number ranging from 0 to 1 using a sigmoid-shape function such as a logistic function. Two different basic processes are involved in a neural network; namely, a training process and a testing process. The neural network will be trained by a back-propagation algorithm (105) using input data (i.e., computer-reported features) and the desired corresponding output data (i.e., biopsy or follow-up proven truth of the malignant or benign status of the mass or microcalcifications in question), for a variety of cases. Once trained, the neural network will accept computer-reported features of the mass or microcalcifications in question and output a value from 0 to 1 where 0 is definitely benign and 1 is definitely malignant. Based on the distribution of these values for various known cases, we will be able to determine what course of action (e.g., biopsy, follow-up or return to normal screening) should be recommended to the radiologist.

## **Results to date**

### **Classification of masses**

Our earlier work showed that a back-propagation, feed-forward artificial neural network could merge human-extracted features of mammographic lesions into a likelihood of malignancy at a similar level of that of an expert mammographer. In the study presented here, however, ANN is used to merge computer-extracted features of mass lesions into a likelihood of malignancy.

The method takes as input the center location of a mass lesion in question. Next, the lesion is segmented from the breast parenchyma (background) using an automatic region growing technique and various features of the lesion are extracted. The automatic lesion segmentation involves the analysis of the size of the grown region as a function of the gray-level interval used for the region growing. Many of the extracted features are determined from a cumulative edge-gradient-orientation histogram analysis modified for orientation relative to a radial angle. Input to an ANN consists of four features from the gradient analysis along with the average gray value within the grown lesion. The gradient measures include the FWHM (full width at half max) of the cumulative edge-gradient-orientation histogram calculated from pixels within the lesion and its neighboring surround, and from just pixels along the lesion margin (see Figures 1-3). These measures correspond to the presence of spiculation, which is a sign of malignancy in the visual interpretation of mammographic masses. The ANN's structure consisted of 5 input units, one hidden layer with 4 hidden units and one output unit. In this task, the output unit ranged from 0 to 1, where 1 corresponded to the lesion being malignant and 0 corresponded to the lesion being benign. Use of ROC analysis with self-consistency testing and round-robin testing was employed as discussed in the previous section.

The classification method was evaluated using a pathologically-confirmed database of 95 masses (57 malignant and 38 benign), of which all but one had been sent to biopsy. The mammograms in the database had been digitized to a pixel size of 0.1 mm. Using the five input features, an Az (area under the ROC curve) of 0.83 was obtained in the task of distinguishing benign from malignant masses using a round-robin method for evaluation. However, we found that by using a rule-based decision

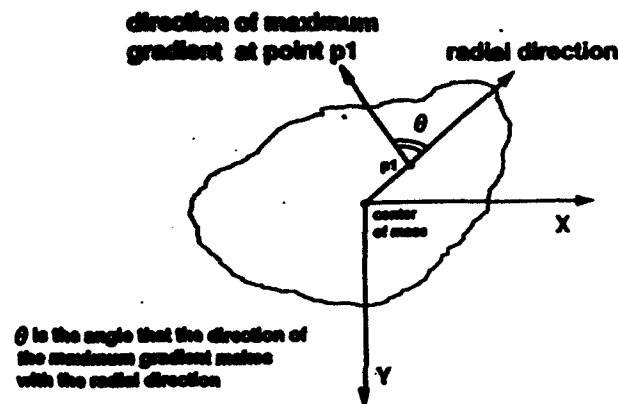


Figure 1. Schematic illustrating the maximum gradient and its direction relative to the radial direction indicated.

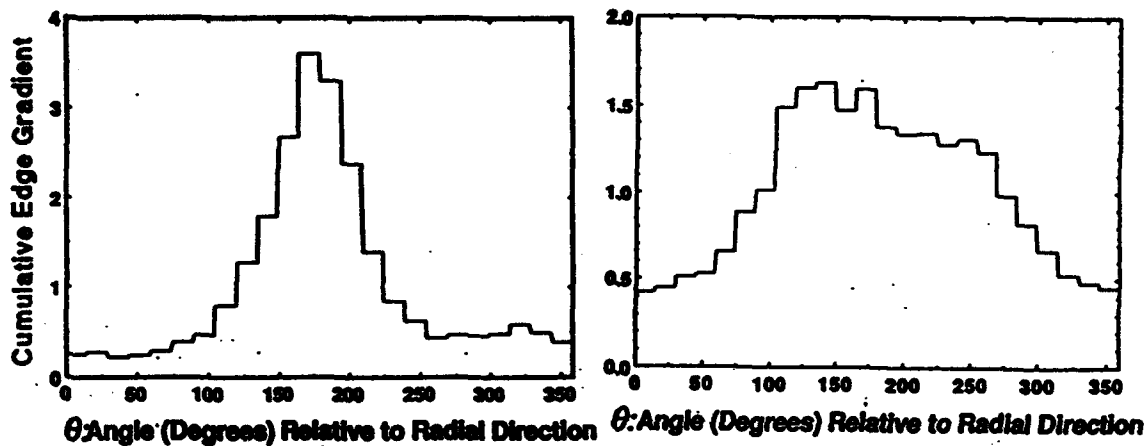


Figure 2. Cumulative edge-gradient-orientation histograms illustrating the presence of (a) a non-spiculated mass as indicated by the relatively narrow peak in the histogram and (b) a spiculated mass as indicated by the presence of a broader peak.

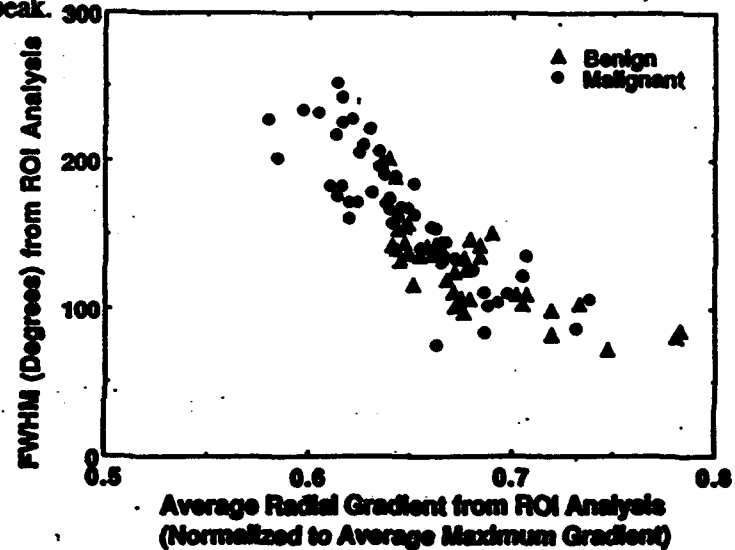


Figure 3. Relationship between FWHM of edge-gradient-orientation histogram and average radial gradient for malignant and benign masses.



on one of the features (FWHM) based on its correspondence to visual interpretation methods, prior to use of the ANN, the performance increased yielding an Az of 0.90 for distinguishing between malignant and benign masses.

## **Results to date**

### **Classification of microcalcifications**

The analysis of microcalcifications can be difficult to perform consistently for human observers leading to the poor positive predictive value. We have been investigating methods to identify computer-extracted quantitative features of microcalcifications and their clusters that can be used to classify malignant and benign clustered microcalcifications, and, to exam if a computer can make accurate differential diagnoses based on computer-extracted features. In this study, features of the microcalcifications and their clusters were automatically extracted from digitized conventional mammograms.

The microcalcifications were segmented using the following method, which is described in detail elsewhere. A third-degree polynomial was fitted to the pixel-value distribution in a ROI (region of interest) of the digitized mammogram in both horizontal and vertical directions to reduce the background structure of the breast parenchyma. The microcalcification was then delineated by region growing. The effective thickness of the microcalcification (physical dimension along x-ray projection line) was estimated from signal contrast (mean pixel value above background) of the isolated microcalcification. This was done by first converting signal contrast in terms of optical density to contrast in terms of exposure using knowledge of the H&D curve of the screen-film system, and secondly converting contrast in terms of exposure to physical dimension using the exponential attenuation law assuming a "standard" model of the breast and the microcalcification. The standard model assumes (i) a 4-cm compressed breast composed of 50% adipose and 50% glandular tissues; (ii) a microcalcification composed of calcium hydroxyapatite with physical density of  $3.06 \text{ g/mm}^3$ ; and (iii) a 20-keV monochromatic x-ray beam. Two contrast corrections were applied for better

accuracy: compensation for blurring caused by the screen-film system and the digitization process, and compensation for x-ray scatter.

The usefulness of the features were evaluated using the distributions of the benign and malignant populations. Features capable of showing separation between benign clusters from the malignant population were chosen for the automated classification. Extracted features were based on the size, shape, contrast, and uniformity of individual microcalcifications; and the size and shape of microcalcification clusters. An artificial neural network was used to classify benign versus malignant clusters of microcalcifications using 8 computer-extracted features. The database consisted of 100 images, digitized at 100-mm pixel size and 10-bit grey-scale resolution, from 53 patients biopsied for suspicion of breast cancer based on clustered microcalcifications. The neural network correctly identified 47% of the benign patients, all of whom had biopsies, and 100% of the malignant patients. We conclude that a computer is capable of distinguishing benign from malignant clustered microcalcifications even at 100-mm pixel size.

## **(2) Development of a dedicated CAD module for use by radiologists.**

### **Experimental methods**

The various computer-vision and artificial intelligence schemes will be incorporated into a dedicated computer system (module) equipped with a high-speed computer and a digital image interface, as shown in Figure 4. The digital image interface will initially be to a film digitizer in order to test the CAD schemes using the large database of clinical mammograms available in our Radiology Department. Later, mammographic images will be obtained using the CR system or the CCD-based digital biopsy unit. The intelligent modular workstation will need to have sufficient computer power (CPU and large capacity memory) and display capabilities to allow for "real-time" computation and viewing of the computer-vision results. Thus, we plan to upgrade our current computer hardware and optimize our software to achieve high-speed and efficient computation of CAD results. Our target is to reduce the

CPU time required for CAD computations from the current level of about 5 minutes per image to a few seconds. Also, appropriate man-machine interfaces will be needed for effective and efficient computer-assisted interpretations. This part of the research will involve the examination of various methods of presenting the computer-determined results to the radiologists. Important parameters include (a) the shape and size of the markers of the computer output that could represent the severity or confidence level (probability) of the lesion, (b) the optimal operating point of the CAD schemes (high sensitivity with an acceptable number of false positives), (c) the timing and duration of displaying the computer output, (d) the selection of the minimum number of inputs required for radiologists and (e) the user-friendliness of instructions and input entries.

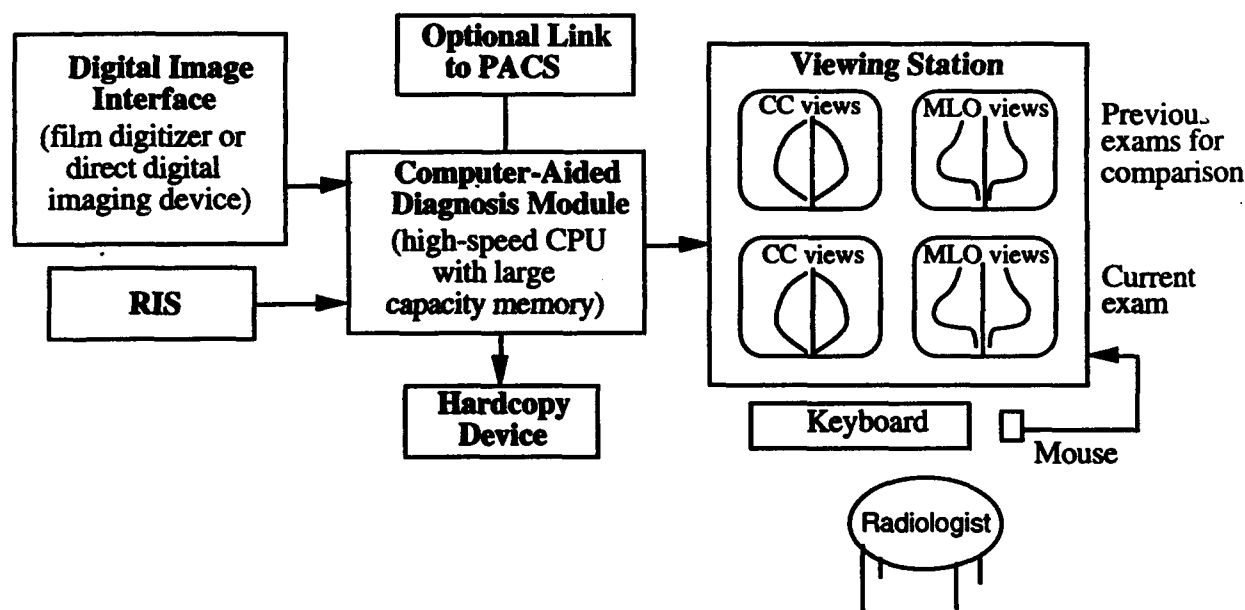


Figure 4. The intelligent modular workstation. The digital image interface will be the film digitizer and also direct digital imaging devices such as the CR system and the digital biopsy unit. The CAD module requires a high-speed CPU and large capacity memory. Hardcopy devices include the laser film printer and the economical thermal-paper image printer. Optional links to RIS (radiology information system) and PACS (picture archival and communication system) are included.

The development of the prototype modular system will be achieved in stages. In Phase 1, the introduction of the computer-vision aid to the radiologists will be implemented with minimum change in the current radiologist method of operating. This will allow for a gradual introduction in order to minimize any resistance to change. Thus, only computer-reported detection results will be presented to

the radiologist, leaving all of the interpretation to the radiologist. Basically, the computer will serve as a "second opinion" indicating suspicious areas without critique as to their degree of malignancy. Original films will be digitized (2048 by 2048 digitization matrix) and analyzed, with the computer output then printed on either film or thermal paper. Radiologists will perform their normal reading using the original image and the computer results. It is believed that this introduction of CAD to radiologists will cause minimum modification to their normal reading patterns, thus allowing for a smooth and effective transition. During Phase 2, results from the classification schemes also will be included, using the methodology described for Phase 1. However, in this second phase the computer will serve as a "second opinion" for both the location and the interpretation of breast lesions.

During the first two phases, we will investigate the best markers for use by radiologists, who may prefer arrows or circles (icon-type symbols). It should be noted that the implementation of computer vision in mammographic screening using the methods described above is not limited to fully digital (PACS) departments but can be incorporated in a general film-based radiology department or in a mobile, filmless mammography unit (i.e., a limited PACS environment).

Once the use of computer vision is shown to be useful, beneficial and efficient, we will incorporate high-resolution, state-of-the-art monitors into the dedicated computer system (Phase 3) as shown in Figure 1. The "intelligent" module will be interfaced to our department's RIS (radiology information system) to link the demographic and medical history information with the CAD output. In order for the radiologist to examine the entire breast image, the display monitor will need to have 2K by 2K capability. In mammography, each breast image usually can be digitized adequately into a 2K by 1K image. Thus, in order to view all four breast images (left and right CC views and left and right MLO views), two high-resolution 2K by 2K monitors are needed. However, in the practice of radiology, films (images) from previous examinations play an important role in the current exam due to the need for comparison in order to detect subtle changes. Thus, the display requirements are four 2K by 2K monitors (in a 2 by 2 arrangement), allowing the top two monitors to be used for sequencing through previous exams of the patient in question. In this phase, the radiologists will do their reading of the mammographic cases from the high-resolution monitors. Due to the dynamic nature of the display, the

computer-reported results can be presented in a toggle format where the radiologist can press a button to either show or remove the computer-reported results. In addition, the computerized schemes can be configured to allow for the radiologist to control the tradeoff between the sensitivity and specificity of the computer output, because more true-positive detections always can be achieved at the cost of a larger number of false-positive findings, and vice versa. This tradeoff would be adjusted by the radiologist, depending on the nature of the case material and personal preference. For example, a radiologist might choose a computer output with high sensitivity for examining high-risk patients, whereas a lower sensitivity and correspondingly lower false-positive rate might be preferred for patients at low risk for cancer. It should be noted, however, that increasing the number of interactive choices available to the radiologist will lengthen the reading time per case. Therefore, we will investigate optimization of the module's human interface by studying the relationship between achievable diagnostic accuracy and required reading time.

### **Results to date**

The computerized image analysis software has been integrated into a user friendly interface based on UNIX, XWINDOWS and Motif and operated on an IBM RISC 6000 Series 570 computer workstation. The prototype (hardware & software) was demonstrated at the 1994 annual meeting of the Radiological Society of North America (RSNA) and was well received by the many radiologists in attendance. Currently, arrows (red for masses and yellow for clustered microcalcifications) are used to indicate the computer-detected location of lesions. The input to the system can be either a film that is digitized and then analysed automatically or a computer file containing a digital image. The prototype system is interfaced to a Konica laser film digitizer which enables digitization of the mammograms to approximately 2K by 2K matrices. Video output of the IBM monitor is connected to a low-resolution thermal printer (approximately 1K by 1K) for hardcopy reporting of the CAD results. The prototype system will be transferred to the clinical reading area for the next phase of development and testing.

### **(3) Evaluation procedure using large clinical databases**

#### **Experimental methods**

As described in the previous section, the computer-vision methods for mammography will be developed in phases. Plans include testing the computer-vision system at the end of each phase in order to demonstrate the effect of the various modes of presentation on the accuracy, efficiency and acceptability of the mammographic aid. The system will be evaluated using clinical mammograms obtained from both a low-risk population and a high-risk population. The low-risk population will be obtained from The University of Chicago mammography screening program. The high-risk population will be drawn from examinations referred to our Department of Radiology, since The University of Chicago serves as a tertiary medical center. Initially, performance studies will be done using a database of preselected mammographic cases that have a distribution of subtle cases of normal, benign and malignant areas of either masses or microcalcifications. Later studies will be performed using a more representative database of consecutive mammographic cases obtained from four weeks worth of screening. "Truth" concerning the presence and malignancy of masses and microcalcifications will be established with the aid of expert mammographers, follow-up reports and surgical biopsy reports. Normal cases will be selected from patients who have had normal follow-up exams. Performance studies will be done using cases involving the four conventional mammograms (left and right CC views, and left and right MLO views), since these are the usual images obtained in screening.

At the detection stage of the computer-vision system, performance will be examined by calculating the fraction of lesions detected (true-positive rate) and the number of falsely-reported areas per case. At the classification stage of the computer-vision system, performance will be examined by calculating the fraction of malignant cases correctly classified (true-positive classification rate) and the number of benign cases that are reported by the computer as being malignant (false-positive classification rate). The clinical database for these performance evaluations will contain 180 cases (60 normal, 30 with benign masses, 30 with malignant masses, 30 with benign microcalcifications, and 30 with malignant microcalcifications).

Observer studies will be performed to examine the usefulness of the computer-assisted interpretation process in enhancing radiologists' performance levels, as compared to the unaided performance by radiologists. During phases 1 and 2, the database cases will be printed with the computer-vision results on each film. These database cases will then be used in observer performance studies. Stratified sampling (106) will be used in choosing subtle cases in order to avoid problems associated with either "too easy" or "too difficult" cases (107). Twelve attending radiologists and senior residents will act as observers. Then, for the 180 cases in the database, three "reading methods" will be tested; (a) the original cases without the computer-vision aid, (b) the cases with the detection-results reported (phase 1 computer locations of suspicious areas) and (c) the cases with both the detection and classification results reported (phase 2 computer locations with probability of malignancy). Each observer will be asked to perform two tasks: (1) locate and rate suspicious areas as to the presence of an abnormality (rating scale of 0 to 100) and (2) indicate an overall level of certainty as to the presence of cancer using a 5-point rating scale where 1=definitely benign and 5=definitely malignant. This five-point scale is the same as that being recommended by the American College of Radiology for routine use by clinical mammographers. The dual-task observer study will allow for evaluation of the utility of both the computer-vision detection and classification results. (In addition, questionnaires will be given to each observer in order to obtain subjective information with regard to the efficiency and acceptability of the computer-vision mammography system.) In the analysis of the observer study results, maximum likelihood estimation (108) will be used to fit a binormal ROC (receiver operating characteristics) curve to each observer's confidence-rating data from each diagnostic method. The index  $A_z$ , which represents the area under a binormal ROC curve, will be calculated for each fitted curve. To represent the average performance of the observers for each diagnostic method, the composite ROC curves will be calculated by averaging the slope and intercept parameters of the individual observer-specific ROC curves. The statistical significance of apparent differences between pairs of diagnostic methods will then be analyzed by applying a "two-tailed" t-test for paired data to the observer-specific  $A_z$  index values.

Free-response ROC (FROC) analysis (109) and FROC-AFROC analysis (110) will be used in analyzing the data pertaining to localization of the abnormality. The ordinates of both FROC curves and AFROC curves are the fraction of lesions (masses or microcalcifications) that are correctly localized by the observer. However, the abscissa of an FROC curve is the average number of false positives per image, whereas the abscissa of an AFROC curve is the probability of obtaining a false-positive image (i.e., an image containing one or more false-positive responses).

After phase 3, another observer study will be performed in which four weeks' worth of mammographic cases will be collected and interpreted by six radiologists with and without the computer-vision results of location and classification. Although this database lacks the control over the subtlety of the cases that the earlier mentioned study has, it represents a more typical clinical situation. Half of the radiologists will read the first two weeks of cases without aid and the second two weeks of cases with the mammographic aid; and the other half of the radiologists will read the first two weeks of cases with the aid and the second two weeks of cases without the aid. Rating methods and analyses will be the same as mentioned above.

### **Results to date**

FROC analysis and ROC analysis has been used extensively for the intermediate testing results of the various detection and classification methods. Constant collection of the database is ongoing. Investigators have developed a case reporting sheet for organizing the new cases on a Macintosh computer using FileMakerPro software. The various databases being collected include pathologically-proven mass and clustered microcalcification cases. In addition, a "missed lesion" database is being digitized in order to test the detection methods in the upcoming grant period. This database includes lesions that were seen in retrospect, i.e., after the cancer was detected at a later date. This database will demonstrate the ability of the detection schemes to increase the sensitivity of detection in a screening program. In a preliminary study (presented at the RSNA 94) in which 26 "missed lesion" cases were analyzed, the computerized detection schemes achieved a sensitivity of 50%. (Note that these "missed lesion" cases can be thought of yielding a sensitivity of 0% when they had been read by the radiologists).



## CONCLUSIONS

Substantial improvements in the performances of the computer-aided diagnosis methods for the detection of masses and clustered microcalcifications have been achieved during the past funding period. For the detection of masses, the sensitivity increased from 85% to 94%, while the false-positive rate per image reduced from 4 to 2.5 per image. For the detection of clustered microcalcifications, the false-positive rate was reduced from 2 per image to approximately 0.7 per image, without loss in sensitivity.

Constant collection of the database is ongoing. Investigators have developed a case reporting sheet for organizing the new cases on a Macintosh computer using FileMakerPro software. The various databases being collected include pathologically-proven mass and clustered microcalcification cases. Databases for both mammograms containing mass lesions and mammograms containing microcalcifications have both increased in size and some have been digitized on more than one digitizer in order to observe the affect of digitization on detection performance. In addition, a "missed lesion" database is being digitized in order to test the detection methods in the upcoming grant period. This database includes lesions that were seen in retrospect, i.e., after the cancer was detected at a later date. This database will demonstrate the ability of the detection schemes to increase the sensitivity of detection in a screening program. In a preliminary study (presented at the RSNA 94) in which 26 "missed lesion" cases were analyzed, the computerized detection schemes achieved a sensitivity of 50%. (Note that these "missed lesion" cases can be thought of yielding a sensitivity of 0% when they had been read by the radiologists).

With regard to the classification of mammographic lesions as an aid in distinguishing between malignant and benign cases, the initial performances for both masses and microcalcifications has been quite promising. In the classification of masses, an Az (area under the ROC curve) of 0.90 was obtained from the ROC analysis of the output from the neural network, which was used to merge the extracted features of the lesions. In the classification of clustered microcalcifications a neural network correctly identified 47% of the benign patients, all of whom had biopsies, and 100% of the malignant patients. We conclude that a computer is capable of distinguishing benign from malignant clustered microcalcifications even at 100- $\mu$ m pixel size.

The computerized image analysis software has been integrated into a user friendly interface based on UNIX, XWINDOWS and Motif and operated on an IBM RISC 6000 Series 570 computer workstation. The prototype (hardware & software) was demonstrated at the 1994 annual meeting of the Radiological Society of North America (RSNA) and was well received by the many radiologists in attendance. The input to the system can be either a film that is digitized and then analysed automatically or a computer file containing a digital image. The prototype system will be transferred to the clinical reading area for the next phase of development and testing.

We are very optimistic about the continuing success of our research. We will continue to improve the detection and classification performance of our algorithms. The mammographers in the clinical reading area of the department are looking forward to the placement of the prototype. Weekly meetings are held between the basic science and clinical researchers in order to ensure a smooth integration of the workstation in the clinical arena.

## REFERENCES

1. Silverberg E, Boring CC, Squires TS: Cancer Statistics, 1990. CA 40: 9-27, 1990.
2. Tabar L, Dean PB: Basic principles of mammographic diagnosis. Diagn. Imag. Clin. Med. 54: 146-157, 1985.
3. American Cancer Society: CA Cancer J Clin 33: 255, 1983.
4. Baker L: CA Cancer J Clin 32: 194, 1982.
5. NCRP Report No. 85: Mammography (National Council on Radiation Protection: Washington, D.C., 1986).
6. Shapiro S, Venet WS, Strax PH, et al.: Ten to fourteen-year effect of screening on breast cancer mortality. JNCI 69: 349-355, 1982.
7. Verbeek ALM, Hendricks JH, Holland R, et al: Reduction of breast cancer mortality through mass screening with modern mammography. Lancet 1: 1222-1224, 1984.
8. Collette HJA, Day NE, et al.: Evaluation of screening for breast cancer in a non-randomized study (the DOM project) by means of a case-control study. Lancet 1: 1224, 1226, 1984.
9. Tabar L, Gad A, Holmberg LH, et al.: Reduction in mortality from breast cancer after mass screening with mammography. Randomized trial from the Breast Screening Working Groups of the Swedish National Board of Health and Welfare. Lancet 1: 829-832, 1985.
10. Andersson I, Aspegren L, Janzon L, et al.: Mammographic screening and nortality from breast cancer: The Malmo mammographic screening trial. Br. Med. J. 297:943,1988.
11. Feig SA: Decreased breast cancer mortality through mammographic screening: Results of clinical trials. Radiology 167: 659-665, 1988.
12. Black JW, Young B: A radiological and pathological study of the incidence of calcifications in diseases of the breast and neoplasms of other tissues. Br. J. Radiol. 58: 596-598, 1965.
13. Wolfe JN: Analysis of 462 breast carcinomas. AJR 121: 846-853, 1974.
14. Sickles EA: Mammographic detectability of breast microcalcifications. AJR 139: 913-918, 1982.
15. Fisher ER, Gregorio RM, Fisher B, et al.: The pathology of invasive breast cancer. Cancer 36: 1-84, 1975.
16. Millis RR, Davis R, Stacey AJ: The detection and significance of calcifications in the breast: A radiological and pathological study. Br. J. Radiol. 49: 12-26, 1976.
17. Murphy WA, DeSchryver-Kecskemeti K: Isolated clustered microcalcifications in the breast: Radiologic-pathologic correlation. Radiology 127: 335-341, 1978.
18. Muir BB, Lamb J, Anderson TJ: Microcalcification and its relationship to cancer of the breast: Experience in a screening clinic. Clin. Radiol. 149: 193-200, 1983.
19. Sickles EA: Mammographic features of 300 consecutive nonpalpable breast cancers. Am J Rad 146: 662-663, 1986.
20. Bassett LW, Gold RH: Breast cancer detection: Mammography and other methods in breast imaging. Grune and Stratton (New York), 1987.
21. Baines CJ, Miller AB, Wall C, McFarlane DV, et al.: Sensitivity and specificity of first screen mammography in the Canadian National Breast Screening Study: A preliminary report from five centers. Radiology 160: 295-298, 1986.
22. Pollei SR, Mettler FA, Bartow SA, Moradian G, Moskowitz M: Occult breast cancer: Prevalence and radiographic detectability. Radiology 163: 459-462, 1987.
23. Andersson I: What can we learn from interval carcinomas? Recent Results in Cancer Research 90: 161-163, 1984.
24. Martin JE, Moskowitz M, Milbrath JR: Breast cancers missed by mammography. AJR 132: 737, 1979.
25. Buchanann JR, Spratt JS, Heuser LS: Tumor growth, doubling times, and the inability of the radiologist to diagnose certain cancers. Radiologic Clinics of North America 21: 115, 1983.
26. Holland T, Mrvunac M, Hendriks JHCL, et al.: So-called interval cancers of the breast. Pathologic and radiographic analysis. Cancer 49:2527, 1982.
27. Tabar L, Dean PB: Teaching Atlas of Mammography, George Thieme Verlag (Stuttgart, New York), 1983.

28. Moskowitz M: Screening for breast cancer: How effective are our tests? A critical review. Ca-A Cancer Journal for Clinicians 33: 26-39, 1983.
29. Winsberg F, Elkin M, Macy J, Bordaz V, Weymouth W: Detection of radiographic abnormalities in mammograms by means of optical scanning and computer analysis. Radiology 89: 211-215, 1967.
30. Spiesberger W: Mammogram inspection by computer. IEEE Transactions on Biomedical Engineering 26: 213-219, 1979.
31. Kimme C, O'Loughlin BJ, Sklansky J: Automatic detection of suspicious abnormalities in breast radiographs. In: Data Structures, Computer Graphics, and Pattern Recognition, edited by A. Klinger, K. S. Fu, T. L. Kunii (Academic Press, New York), 1975, pp. 427-447.
32. Hand W, Semmlow JL, Ackerman LV, Alcorn FS: Computer screening of xeromammograms: A technique for defining suspicious areas of the breast. Computers and Biomedical Research 12: 445-460, 1979.
33. Semmlow JL, Shadagoppan A, Ackerman LV, Hand W, Alcorn FS: A fully automated system for screening xeromammograms. Computers and Biomedical Research 13: 350-362, 1980.
34. Ackerman LV, Gose EE: Breast lesion classification by computer and xeroradiography. Cancer 30: 1025-1035, 1972.
35. Ackerman LV, Mucciardi AN, Gose EE, Alcorn FS: Classification of benign and malignant breast tumors on the basis of 36 radiographic properties. Cancer 31: 342-352, 1973.
36. Wee WG, Moskowitz M, Chang N-C, Ting Y-C, Pemmeraju S: Evaluation of mammographic calcifications using a computer program. Radiology 116: 717-720, 1975.
37. Fox SH, Pujare UM, Wee WG, Moskowitz M, Hutter RVP: A computer analysis of mammographic microcalcifications: Global approach. Proc. IEEE 5th International Conf. on Pattern Recognition: 624-631, 1980.
38. Magnin JE, Cluzeau F, Odet CL, Bremond A: Mammographic texture analysis: an evaluation of risk for developing breast cancer. Optical Engineering 25: 780-784, 1986.
39. Caldwell CB, Stapleton SJ, Holdsworth DW, Jong RA, Weiser WJ, Cooke G, Yaffe MJ: Characterization of mammographic parenchymal pattern by fractal dimensions. Phys. Med. Biol. 35: 235-247, 1990.
40. Fam BW, Olson SL, Winter PF, Scholz FJ: Algorithm for the detection of fine clustered calcifications on film mammograms. Radiology 169: 333-337, 1988.
41. Olson SL, Fam BW, Winter PF, Scholz FJ, Lee AK, Gordon SE: Breast calcifications: Analysis of imaging properties. Radiology 169: 329-331, 1988.
42. Davies DH, Dance DR: Automatic computer detection of clustered calcifications in digital mammograms. Phys. Med. Biol. 35: 111-118, 1990.
43. Astley S, Taylor C, Boggis C, Wilson M, Ellison T: Automated detection of abnormalities on screening mammograms. Radiology 177(P):288, 1990.
44. Grimaud M, Muller S, Meyer F: Automated detection of microcalcifications in mammograms. Radiology 177(P):288, 1990.
45. Jin H-R, Matsumoto K, Kobatake H: Automatic diagnosis of breast cancer with structural line analysis and mathematical morphology. Radiology 177(P) 319, 1990.
46. Karssemeijer N: A stochastic method for automated detection of microcalcifications in digital mammograms. Information Processing in Medical Imaging, Springer-Verlag (New York), pp. 227-238, 1991.
47. Lai SM, Li X, Bischof WF: On techniques for detecting circumscribed masses in mammograms. IEEE Transactions on Medical Imaging 8: 377-386, 1989.
48. Brzakovic D, Luo XM, Brzakovic P: An approach to automated detection of tumors in mammograms. IEEE Transactions on Medical Imaging 9: 233-241, 1990.
49. Gale AG, Roebuck EJ, Riley P, Worthington BS, et al.: Computer aids to mammographic diagnosis. British Journal of Radiology 60: 887-891, 1987.
50. Getty DJ, Pickett RM, D'Orsi CJ, Swets JA: Enhanced interpretation of diagnostic images. Invest. Radiol. 23: 240-252, 1988.
51. Swett HA, Miller PA: ICON: A computer-based approach to differential diagnosis in radiology. Radiology 163: 555-558, 1987.

52. Swett HA, Fisher PR, Cohn AI, Miller PI, Mutalik PG: Expert system controlled image display. Radiology 172: 487-493, 1989.
53. Chan HP, Doi K, Galhotra S, Vyborny CJ, MacMahon H, Jokich PM: Image feature analysis and computer-aided diagnosis in digital radiography. 1. Automated detection of microcalcifications in mammography. Med Phys 14: 538-548, 1987.
54. Chan HP, Doi K, Vyborny CJ, Lam KL, Schmidt RA: Computer-aided detection of microcalcifications in mammograms: Methodology and preliminary clinical study. Invest Radiol 23: 664-671, 1988.
55. Chan HP, Doi K, Vyborny CJ, Schmidt RA, Metz CE, Lam KL, Ogura T, Wu Y, MacMahon H: Improvement in radiologists' detection of clustered microcalcifications on mammograms: The Potential of computer-aided diagnosis. Invest Radiol 25: 1102-1110, 1990.
56. Nishikawa RM, Doi K, Giger ML, Yoshimura H, Wu Y, Vyborny CJ, Schmidt RA, Chan HP: Use of morphological filters in the computerized detection of microcalcifications in digital mammograms. Medical Physics 17: 524, 1990.
57. Nishikawa RM, Giger ML, Doi K, Schmidt RA, Vyborny CJ: Automated detection of microcalcifications on mammograms: New feature-extraction techniques with morphologic filters. Radiology 177(P): 288, 1990.
58. Nishikawa RM, Giger ML, Doi K, Vyborny CJ, Schmidt RA: Computer-aided detection of clustered microcalcifications on digital mammograms. Medical and Biological Engineering and Computing (submitted), 1992.
59. Wu Y, Doi K, Giger ML, Nishikawa RM: Computerized detection of clustered microcalcifications in digital mammograms: applications of artificial neural networks. Radiology (in press) 1992.
60. Giger ML, Yin F-F, Doi K, Metz CE, Schmidt RA, Vyborny CJ: Investigation of methods for the computerized detection and analysis of mammographic masses. Proc. SPIE 1233: 183-184, 1990.
61. Yin F-F, Giger ML, Doi K, Metz CE, Vyborny CJ, Schmidt RA: Computerized detection of masses in digital mammograms: Analysis of bilateral-subtraction images. Medical Physics 18: 955-963, 1991.
62. Yin F-F, Giger ML, Doi K, Vyborny CJ, Schmidt RA: Computerized detection of masses in digital mammograms: Investigation of feature-extraction techniques. Med Phys (submitted) 1992.
63. Wu Y, Giger ML, Doi K, Vyborny CJ, Schmidt RA, Metz CE: Application of neural networks in mammography: Applications in decision making in the diagnosis of breast cancer. Radiology (submitted) 1992.
64. Giger ML, Nishikawa RM, Doi K, Yin FF, Vyborny CJ, Schmidt RA, Metz CE, Wu Y, MacMahon H, Yoshimura H: Development of a "smart" workstation for use in mammography. Proc. SPIE 1445: 101-103, 1991.
65. Doi K, Giger ML, MacMahon H, Hoffmann KR, et al.: Computer-aided diagnosis: development of automated schemes for quantitative analysis of radiographic images. Seminars in Ultrasound, CT and MR (in press).
66. Giger ML, Doi K, MacMahon H, Nishikawa RM, Hofmann KR, et al.: An "intelligent" workstation for computer-aided diagnosis". RadioGraphics (submitted) 1992.
67. MacMahon H, Doi K, Chan HP, Giger ML, Katsuragawa S, Nakamori N: Computer-aided diagnosis in chest radiology. J Thoracic Imaging 5: 67-76, 1990.
68. Metz CE: ROC methodology in radiologic imaging. Invest Radiol 21: 720-733, 1986.
69. Giger ML, Doi K, MacMahon H: Image feature analysis and computer-aided diagnosis in digital radiography. 3. Automated detection of nodules in peripheral lung fields. Med. Phys. 15: 158-166, 1988.
70. Giger ML, Ahn N, Doi K, MacMahon H, Metz CE: Computerized detection of pulmonary nodules in digital chest images: Use of morphological filters in reducing false-positive detections. Med Phys 17: 861-865, 1990.
71. Giger ML, Doi K, MacMahon H, Metz CE, Yin FF: Computer-aided detection of pulmonary nodules in digital chest images. RadioGraphics 10: 41-52, 1990.
72. Yoshimura H, Giger ML, Doi K, MacMahon H, Montner SM: Computerized scheme for the detection of pulmonary nodules: A nonlinear filtering technique. Invest Radiol 27: 124-129, 1992.

73. Katsuragawa K, Doi K, et al.: Image feature analysis and computer-aided diagnosis in digital radiography: Effect of digital parameters on the accuracy of computerized analysis of interstitial disease in digital chest radiographs. Med Phys 17: 72078, 1990.
74. Katsuragawa S, Doi K, et al.: Quantitative computer-aided analysis of lung texture in chest radiographs. RadioGraphics 10: 257-269, 1990.
75. Nakamori N, Doi K, Sabeti V, MacMahon H: Image feature analysis and computer-aided diagnosis in digital radiography: Automated analysis of sizes of hearts and lung in digital chest images. Med Phys 17: 342-350, 1990.
76. Fujita H, Doi K, Giger ML, Chan HP: Investigation of basic imaging properties in digital radiography. 5. Characteristic curves of I.I.-TV digital systems. Medical Physics 13: 13-18, 1986.
77. Giger ML: Film digitization—technical requirements. Invited for presentation. In: Proceedings of Chest Imaging Conference '87, (Eds.) Peppler W, Alter A, Medical Physics Publishing Corp. Madison, Wisconsin, pp. 92-100, 1988.
78. Giger ML, Doi K: Investigation of basic imaging properties in digital radiography. 1. Modulation transfer function. Medical Physics 11: 287-295, 1984.
79. Fujita H, Doi K, Giger ML: Investigation of basic imaging properties in digital radiography. 6. MTFs of I.I.-TV digital systems. Med Phys 12: 713-729, 1985.
80. Fujita H, Giger ML, Doi K: Investigation of basic imaging properties in digital radiography. 12. Effect of matrix configuration on system resolution. Medical Physics 15: 384-390, 1988.
81. Fraser RG, Sanders C, Barnes GT, MacMahon H, Giger ML, Doi K, Templeton AW, Cox GG, Dwyer SJ, Merritt C, Jones J: Digital imaging of the chest: state of the art. Radiology 171: 297-307, 1989.
82. Cook LT, Giger ML, Batnitzky S, Wetzel LH, Murphey MD: Digitized film radiography. Investigative Radiology 24: 910-916, 1989.
83. Montner S, Xu X-W, Tsuzaka M, Doi K, MacMahon H, Yoshimura H, Sanada S, Giger ML, Yin F-F: Evaluation of basic imaging properties of a new digital chest system. Proc. SPIE 1231: 390-393, 1990.
84. Sanada S, Doi K, Xu X-W, Yin F-F, Giger ML, MacMahon H: Comparison of imaging properties of a computed radiography system and screen-film systems. Medical Physics (submitted).
85. Yin F-F, Giger ML, Doi K: Measurement of the presampling MTF of film digitizers using a curve fitting technique. Medical Physics (in press).
86. Yin FF, Giger ML, Doi K, Yoshimura H, Xu XW, Nishikawa RM: Evaluation of imaging properties of a laser film digitizer. Phys. Med. Biol. 37: 273-280, 1992.
87. Giger ML, Doi K, Metz CE: Investigation of basic imaging properties in digital radiography. 2. Noise Wiener Spectrum. Medical Physics 11: 797-805, 1984.
88. Giger ML, Doi K, Fujita H: Investigation of basic imaging properties in digital radiography. 7. Noise Wiener spectra of I.I.-TV digital imaging systems. Medical Physics 13: 131-138, 1986.
89. Giger ML, Ohara K, Doi K: Effect of quantization on digitized noise and detection of low-contrast objects. Proc. SPIE 626: 214-224, 1986.
90. Kume Y, Doi K, Ohara K, Giger ML: Investigation of basic imaging properties in digital radiography. 10. Structure mottle of I.I.-TV digital imaging systems. Medical Physics 13: 843-849, 1986.
91. Giger ML: Image quality: Effects of digitization, matrix size and noise. Invited for presentation at the 1987 AAPM Annual Summer School, In: Image Communication and Image Analysis. (Mulvaney, Haus, Windham, eds.), New York, AIP (in press).
92. Giger ML, Doi K: Investigation of basic imaging properties in digital radiography. 3. Effect of Pixel Size on SNR and Threshold Contrast. Med. Phys. 12: 201-208, 1985.
93. Giger ML, Doi K: Effect of pixel size on detectability of low-contrast signals in digital radiography. J of the Optical Society of America A 4: 966-975, 1987.
94. Ohara K, Chan HP, Doi K, Giger ML, Fujita H: Investigation of basic imaging properties in digital radiography. 8. Detection of simulated low-contrast objects in DSA images. Medical Physics 13: 304-311, 1986.

95. Ohara K, Doi K, Metz CE, Giger ML: Investigation of basic imaging properties in digital radiography. 13. Effect of structured noise on the detectability of simulated stenotic lesions. Medical Physics 16:14-21, 1989.
96. MacMahon H, Metz CE, Doi K, Kim T, Giger ML, Chan H-P: The effect of display format on diagnostic accuracy in digital chest radiography: A comparison of hardcopy, video, and reversed grey scale. Radiology 168: 669-673, 1988.
97. MacMahon H, Doi K, Sanada S, Montner SM, Giger ML, et al.: Effect of data compression on diagnostic accuracy in digital chest radiography. An ROC study. Radiology (submitted).
98. MacMahon H, Sanada S, Doi K, Giger ML, Xu X-W, Yin F-F, Montner SM, Carlin M: Direct comparison of conventional and computed radiography with a dual image recording technique. RadioGraphics (submitted).
99. Asada N, Doi K, MacMahon H, Montner S, Giger ML, Abe C, Wu Y: Potential usefulness of artificial neural network for differential diagnosis of interstitial lung diseases: a pilot study. Radiology (in press).
100. Murphy WA Jr, Destouet JM, Monsees BS: Professional quality assurance for mammography screening programs. Radiology 175: 319-320, 1990.
101. Bird RE: Professional quality assurance for mammography screening programs. Radiology 177: 587, 1990.
102. Brenner RJ: Medicolegal aspects of breast imaging: variable standards of care relating to different types of practice. AJR 156: 719-723, 1991.
103. Pratt WK: Digital Image Processing (Wiley, New York, 1978).
104. Serra J: Image Analysis and Mathematical Morphology, (Academic Press, New York), 1982.
105. Rumelhart DE, Hinton GE, Williams RJ: Learning internal representations by error propagation. In: Rumelhart DE, McClelland JL, PDP Research Group. Parallel distributed processing: Explorations in the microstructure of cognition. Cambridge: MIT Press 1: 318-362, 1986.
106. Kendall M, Stuart A: The Advanced Theory of Statistics, Vol. 3 (Hufner, New York), 1976.
107. Metz CE: Some practical issues of experimental design and data analysis in radiological ROC studies. Invest. Radiol. 24: 234-245, 1989.
108. Dorfman DD, Alf E: Maximum likelihood estimation of parameters of signal detection theory and determination of confidence intervals-rating method data. J Math Psych 6: 487-498, 1969.
109. Bunch PC, Hamilton JF, et al.: A free response approach to the measurement and characterization of radiographic observer performance. Proc. SPIE 127: 124-135, 1977.
110. Chakraborty D: Maximum likelihood analysis of free-response receiver operating characteristic (FROC) data. Med. Phys. 16: 561-568, 1989.